BBAA VI International Colloquium on:
Bluff Bodies Aerodynamics & Applications
Milano, Italy, July, 20-24 2008

# NUMERICAL INVESTIGATION OF THE FLOW AROUND A RECTANGULAR CYLINDER NEAR A SOLID WALL

**Stefano Malavasi[*], Nicola Trabucchi[†]**

[*] Dept. of I.I.A.R.
Politecnico di Milano, piazza Leonardo da Vinci 32, 20133 Milano, Italy
e-mail: Stefano.Malavasi@polimi.it,

[†] Dept. of I.I.A.R.
Politecnico di Milano, piazza Leonardo da Vinci 32, 20133 Milano, Italy
e-mail: Nicola.Trabucchi@mail.polimi.it,

**Keywords:** CFD, rectangular cylinder, force coefficients, mean flow structure, asymmetrical bounded flow.

***Abstract.*** *The bounding effect of an asymmetrical confined flow around a rectangular cylinder immersed in a water steady flow is analyzed with opportune numerical simulations. The phenomenon considered is characterized by the presence of a high distortion of the vortex structures around the cylinder, which are the main responsible of the particular trend of the hydrodynamic coefficient experimentally highlighted in this conditions. In order to deep investigate and integrate the experimental evidence, we have numerical simulated the experimental setup. The results in terms of mean field characterization and pressure distribution allow to obtain further information for the interpretation of the phenomena.*

## 1 INTRODUCTION

The study of flow around bluff bodies of rectangular shape has a deep engineering interest because many civil but also industrial structure can be assimilate to this shape. The fluid-dynamic forces acting on a rectangular cylinder have been mainly investigated for unbounded flow conditions. In particular from these studies one learns about the flow characteristic around deck sections of long span bridges and tall buildings. These studies are important in terms of aerodynamic design to investigate the structure aerodynamic features in detail.

Even the bounding effect of a fixed wall occurs in many application of civil engineering, for example in the case of bridges and/or buildings placed in the proximity of other structures or particular land morphology, both in water or in air-flow. This condition is very important in an engineering point of view and needs to be explored in detail. Despite the simple geometry of the considered model and the wide practical use of cylindrical structures with rectangular cross-section, most research studies on the effect of bounding condition are concerned with structures of circular and square cross section.

The literature works on circular and square cross-sections are quite wide investigated and the physics of the flow is well described. For its completeness and for the analogies on the configuration here considered, we have selected the studies of Martinuzzi et al. [9] and Straatman and Martinuzzi [11, 12]. In the fist paper, they performed a series of wind tunnel experiments

collecting mean and fluctuating surface pressure data for a square cylinder placed near a solid wall at Re = 18900. Moreover, they provided a complete study of the influence of a wall on the flow around a square cylinder, both with experimental and numerical analysis. The detailed measurements of surface pressure distribution on the cylinder faces and the bottom wall allows finding different flow regimes in the gap flow (between the cylinder bottom face and the wall). The definition of flow regimes done by Martinuzzi et al. [9] give a key lecture of the analysis of some of experimental data on the rectangular cylinder collected by Malavasi and Guadagnini [1] which dealt with the interaction between a free-surface flow and a rectangular cylinder discussing the mean hydrodynamic coefficients and the vortex shedding frequencies of the phenomenon.

Experimental works on rectangular cylinder immersed in asymmetrical bounded flow are also provided by Blois and Malavasi [3] which investigated the flow field structures involved in the same experimental configuration of [1] with a PIV technique and Cigada et al. [2] which studied the effect that the presence of a wall induces on the fluid dynamic loading affecting a rectangular cylinder placed in a wind tunnel at several elevations from the wall itself. Numerical studies on rectangular cylinder are available for unbounded or symmetrical bounded flow conditions (e.g. Shimada and Ishihara [5] and Yu and Kareem [6]). The numerical results of Shimada and Ishihara [5] have been considered as reference for the numerical validations of the CFD commercial code here used.

In present work, we discussed about a first series of numerical simulations provided in order to collect information about different aspects of the influence that the presence of a confining wall exerts on the flow mechanism around the rectangular cylinder. The flow is characterized by means of mean hydrodynamic coefficients, mean flow field visualizations and pressure distribution, both around the obstacle and along the bottom wall. We provided an extensive comparison with the experimental results in terms of force coefficients and dimensionless parameters which characterize the structure of the mean flow around the obstacle; moreover we used the additional data offered by the numerical approach to help in the phenomenon comprehension.

## 2 VALIDATION OF THE NUMERICAL MODEL

The simulation of the study cases are performed using the commercial CFD code FLOW-3D®. It solves the Reynolds averaged Navier-Stokes (RANS) in the time dependent form, usually called Unsteady RANS in CFD theory. This particular approach has gained interest in the recent years for the increasing advance in computing power and efficiency of numerical procedures. As it is reported in Iaccarino *et.al*. [12] the unsteady RANS provide good quantitative and qualitative agreement with experimental data for flows which exhibit characteristics common to all flows past bluff obstacles, including separation and large scale unsteadiness. For a preliminary check of the numerical setup used in our analysis, we dealt with the reproduction of a relevant literature unbounded test case. For the completeness of the available parameters of comparison and the similarity of the numerical algorithm (**Tab. 1**), we have chosen the investigation of Shimada and Ishihara [5]: indeed the Authors studied the aerodynamics characteristics of rectangular cross-sections.

| | *Shimada and Ishihara [5]* | *Present Work* |
|---|---|---|
| **basic equation** | Unsteady RANS | Unsteady RANS |
| **model** | 2D | 3D |
| **turbulence model** | k-e model (KaLa modification) | RNG k-e model |
| **near-wall treatment** | two-layer model | equilibrium wall function |
| **time - marching** | first order implicit scheme | first order explicit scheme |
| **convective term** | third order | third order |

Tab. 1: Numerical characteristics of test model [5] and present model.

**In the modeling of this case we start by setting the geometry and inflow boundary in a proper way in order to achieve the same Re of flow simulated in Shimada and Ishihara [5]. In particular, we have decided to use the same cylinder geometry employed in the experimental campaign of DIIAR ([1] [2] [3]) and then we have calculate the opportune inflow velocity $U_0$ in order to reproduce the same Re used in [5]. In the outflow section we have used a continuative boundary condition which allows a smooth prosecution of the flow across the boundary employing a zero-derivatives of all the numerical quantities simulated involved in the flow. In the spanwise and vertical direction symmetric condition are imposed. In**

**Fig. 1**) a useful representation of the analytic domain employed is shown.

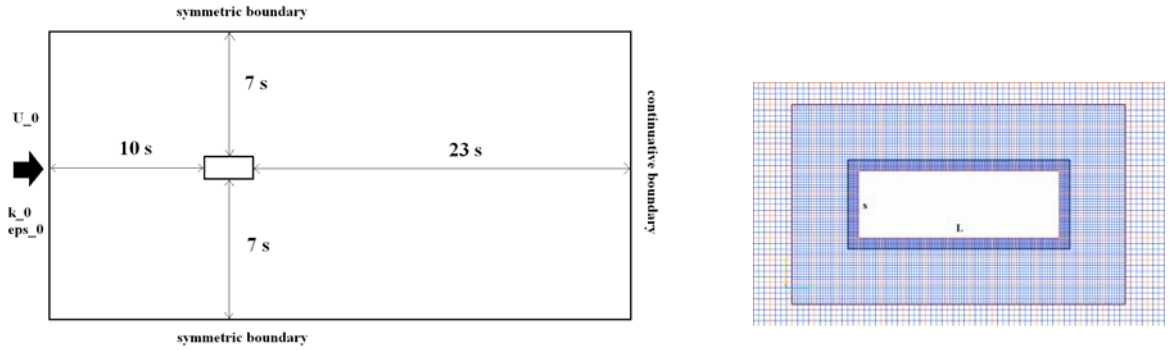


Fig. 1: Analytic domain and boundary conditions of unbounded test case reproduction

To proper model this condition we exploit a multi-gridding approach by refining the mesh blocks around the obstacle. The results of the simulation has showed very good results: from the temporal series of force coefficient reported in **Fig. 2**) we have calculated the mean values; moreover from a spectral analysis of the lift signal we have also calculate the frequency f of the vortex shedding (the calculate value is f = 1.016 Hz) from a, corresponding to Strouhal number St = 0.165. A summary of the comparison is reported in Tab.(2)

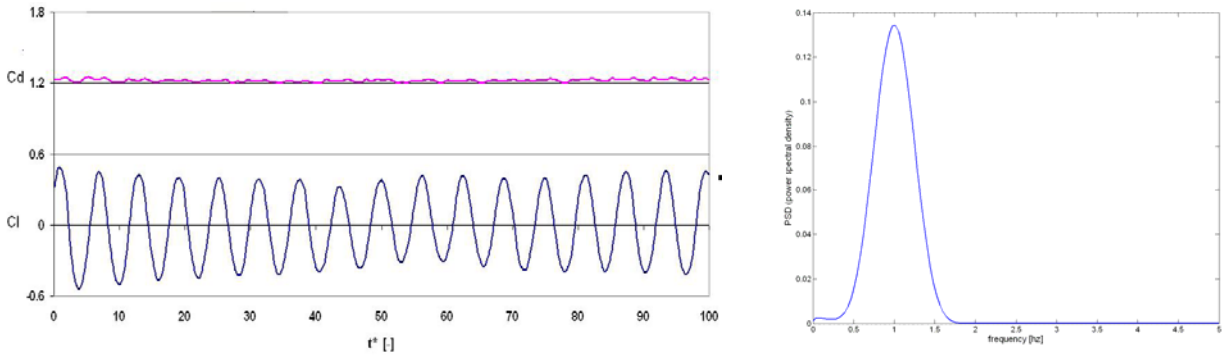


Fig. 2: (a) Time history of force coefficient, where $t^*=(t \cdot U_0)/s$ is the dimensionless simulation time; (b) power spectra of $C_L$

| | Shimada and Ishihara [5] | Present work |
|---|---|---|
| $C_D$ | 1.200 | 1.221 |
| $S_t$ | 0.165 | 0.165 |
| $C'_L$ | 0.221 | 0.296 |

Tab. 2 Comparison between the results of Shimada and Ishihara [5] and present work.

The good reproduction of the aerodynamic of the cylinder in unbounded is used to proper define the spatial discretisation needed for a correct development of the turbulent structures near the body. The approach using RNG k-ε seem to be suitable for the analysis in present work; moreover literature reference, for example Younis and Przulj [7] certificates how it is likely that RNG model yields improvements in the prediction of separated flow as in bluff bodies.

It is immediate to realize that the condition set up of Fig.(1) is quite different from the experimental conditions in the laboratorial campaign at DIIAR, depicted in Fig.(3)

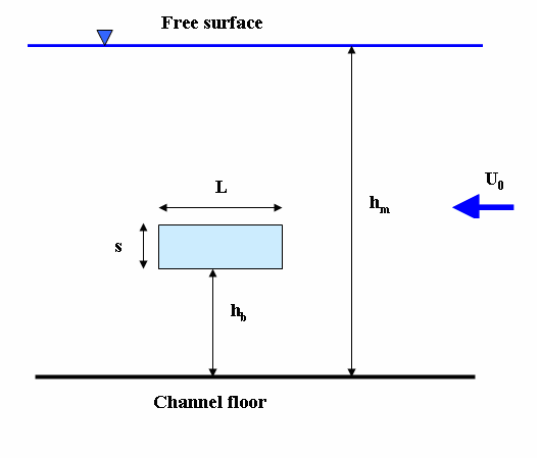


Fig. 3: Experimental Configuration

So next step in the validation of the numerical approach has the aim to check the settings used in the numerical reproduction of the experimental setup.

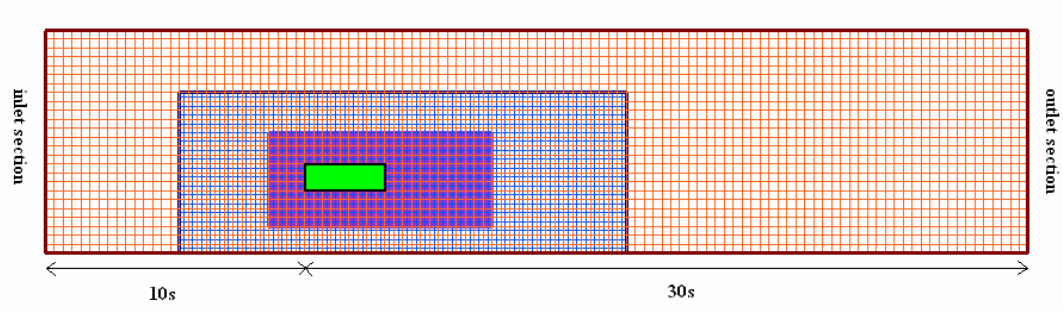


Fig. 4: Numerical setup for the reproduction of experimental configuration

We decided to simulate the free-surface flow even in the numerical model using the Tru-VOF numerical algorithm available in the commercial code used in present work. Sketch of the multi-gridding discretisation of the numerical model is reported in Fig.(4): it has been utilized for all the $h_b/s$ ratio considered in present work and a standard simulation procedure has been employed. A preliminary simulation is used to reproduce an opportune velocity profile with the boundary layer of the experimental condition ($\delta/s \approx 1$). This has been then set as the inflow boundary at the inlet section, while a water level $h_m = 0.42$ m is provided in order to ensure the same experimental volumetric flow rate. In the outlet section a pressure condition is used. The turbulence quantities at the inlet are derived from the value of turbulence experimentally evaluated (Tu = 14%). From these values we have deduced the correspondent value of turbulent kinetic energy employing the isotropic turbulence relation:

$$k_0 = \frac{3}{2}(T_u U_0)^2 \tag{1}$$

An estimate for the dissipation rate ε was obtained from the following formula proposed in Straatman and Martinuzzi [11]:

$$\varepsilon_0 = \frac{0.61 \cdot k_0^{\frac{3}{2}}}{5 \cdot s} \tag{2}$$

We decided to use as reference test the hydraulic condition $h^* = 5$ and $h_b/s = 2.33$. In this condition characteristics similar to the unbounded flow condition were experimentally found, as reported in Malavasi and Guadagnini [1] and in Blois and Malavasi [3]. This similarity has encouraged a wide study about this condition, for which we have a large experimental database both in term of hydrodynamic coefficients and PIV mean flow field for various submergence condition. For the reproduction of this experimental condition the main parameters used in the simulation are reported in Tab.(3)

| $U_0$ [m/s] | $h_m$ [m] | $k_0$ | $\varepsilon_0$ |
|---|---|---|---|
| 0.197 | 0.445 | 0.0115 | 0.0008 |

Tab. 3: Hydraulic and numerical parameters of the experimental test case simulation

For the determination of mean flow magnitudes, the numerical data have been extracted from the time history of the simulated data when a steady state solution has been reached. As suggested by the user manual of FLOW-3D®, a little variation (less than 1%) of relevant global parameters as the turbulent kinetic energy is a reliable indication of the steady state. Notwithstanding, in our work we decided to extend the simulation time after that this condition has been reached, to collect an opportune time history of all the simulated parameters. As it is suggested in Iaccarino *et.al* [12], employing unsteady RANS solver, a time averaged solution can be computed over duration of four periodic cycles of the simulated vortex shedding. In present work the simulation time has been regulated in order to achieve at least four oscillating cycles of vortex shedding. The comparison of the mean hydrodynamic coefficient showed good results, even considering the high uncertainty associated with measurements of low Reynolds number (Tab. 4).

| | **Drag Coefficient** | **Lift Coefficient** |
|---|---|---|
| Malavasi and Guadagnini [1] (Experimental) | 1.574 [0.18] | -0.023 [0.24] |
| Present work (Numerical) | 1.461 | 0.155 |

Tab. 4: Comparison of mean hydrodynamic coefficient ([uncertainty]).

After the check of the global values of loading on the cylinder, we dealt with the evaluation of the mean flow field. To do this the instantaneous numerical velocity fields in the symmetry plane of the numerical model has been averaged over the same simulated time interval from which we have derived the force coefficients (Fig.5).

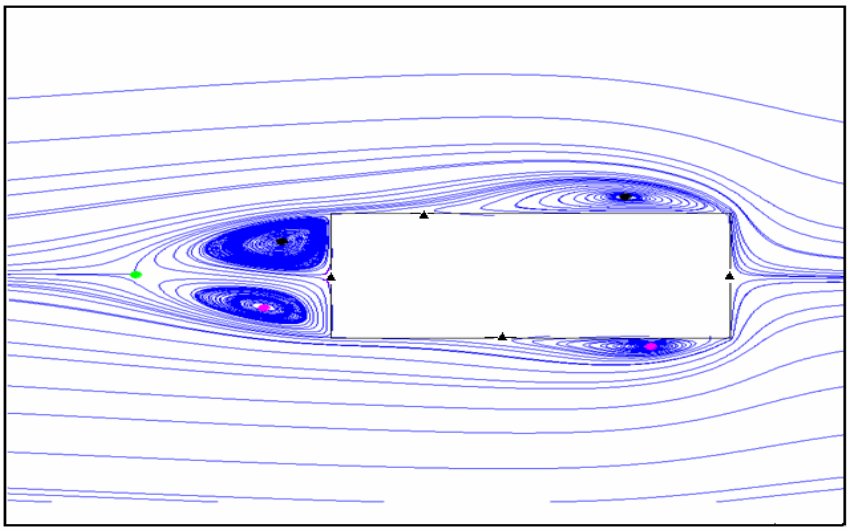

Fig.5: Mean flow structures ($h_b/s$=2.33, h*=5); ●, anticlockwise vortex; ■, clockwise vortex; ▲, saddle points. (Present work)

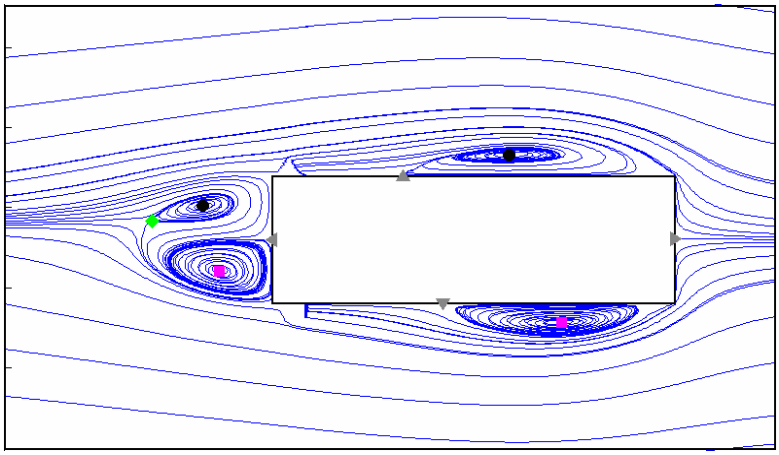

Fig.6: Mean flow structures ($h_b/s$=2.33, h*=5); ●, anticlockwise vortex; ■, clockwise vortex; ▲, saddle points. (Blois and Malavasi [3])

A quantitative comparison between numerical and experimental mean flow structure was provided by the post-processing of the numerical simulated velocity fields. We used the feature-based approach applied by Blois and Malavasi [3] on the PIV data (Fig.6). Significant lines are extrapolated from 2D flow fields decoupling the horizontal information from the vertical one by localizing the position where the sign of the velocity component changes: these lines allow finding relevant point in the flow field as vortex centre, reattachment and stagnation points. With reference to Fig.(7), in the frontal region the stagnation point is characterized with the parameter Q*, defined as $Q^* = Y_{SP} / s$ (where $Y_{SP}$ is the vertical distance of the stagnation point from the horizontal plane y= 0). In the base region the parameter $Lf^*$, defined as Lf /s, is used to define the elongation of the formation region downstream the base cylinder surface (where Lf is the distance of the point where the vertical profile of horizontal velocity presents only positive values of velocity). In lateral regions the parameters $D^*_{bi} = D_{bi}/s$ and $D^*_{be} = D_{bi}/s$ which provides a measure of the transversal width of the shear layer respectively at the extrados and intrados of the cylinder while the reattachment point is defined by the parameters $R^*_{bi} = R_{bi}/s$ and $R^*_{be} = R_{bi}/s$.

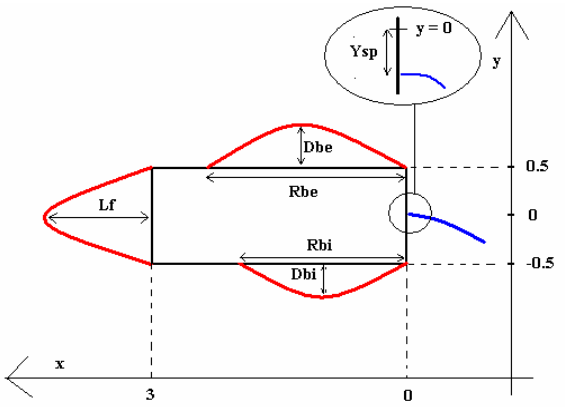


Fig. 7: Sketch of the characteristics sizes of mean flow field structures.

Tab.(5) reports the comparison between the numerical flow filed and the results obtained from the PIV data collected in the same hydraulic condition by Blois and Malavasi [3].

| $h_b/s = 2.33$ | Q* | $R_{be}$* | $D_{be}$* | $R_{bi}$* | $D_{bi}$* | Lf |
|---|---|---|---|---|---|---|
| Present Work | 0.020 | 2.167 | 0.150 | 1.733 | 0.108 | 1.433 |
| Blois and Malavasi [3] | 0.010 | 2.030 | 0.166 | 1.730 | 0.146 | 1.180 |

Tab. 5: Comparison of the geometrical characteristics of mean flow field.

We highlight good correspondence between the numerical and experimental test. We note a slight overestimation of the reattachment length (more accentuated in the extrados region) and of formation length in the base region; on the contrary, the vertical dimension of the recirculation zone in the lateral region is underestimated. The over all correct reproduction of the vortex structures around the obstacle ensure the reliability of the numerical schematization, in particular in term of mesh resolution and boundary condition. These results allow us to use the numerical approach to deal with simulation of small elevation cases with the aim of extend and complete the experimental range of analysis.

## 3 RESULTS

The validated numerical model and the simulation procedure tested in the previous section are used in the analysis of the study cases of present work. In particular the aim of these simulations is to improve the information about the influence that presence of a confining wall exerts on the flow mechanism around the rectangular cylinder. The flow is characterized by means of mean hydrodynamic coefficients, mean flow field visualization and pressure distribution, both around the obstacle and along the bottom wall. With reference to Fig.(3), the main hydraulic parameters of the experimental condition numerical reproduced are a constant value of $h_m$ = 0.42m, which leads to maintain the blockage coefficient constant using the same obstacle; The elevation cases numerical simulated are: $h_b/s$ = 2, 1.5, 1, 0.5.

Fig.(8) shows the flow field numerically simulated at different elevations of the cylinder. With the progressive reduction of $h_b/s$ a reduction of the formation bubble at the intrados is noted, with the complete disappearance of the formation bubble for the smallest elevation considered; on the contrary a progressive increase of the formation bubble at the extrados is evident. In all the condition tested the mean flow reattaches along the sides of the cylinder, even if for $h_b/s$ = 0.5 the reattachment point at the extrados is very close to the trailing edge.

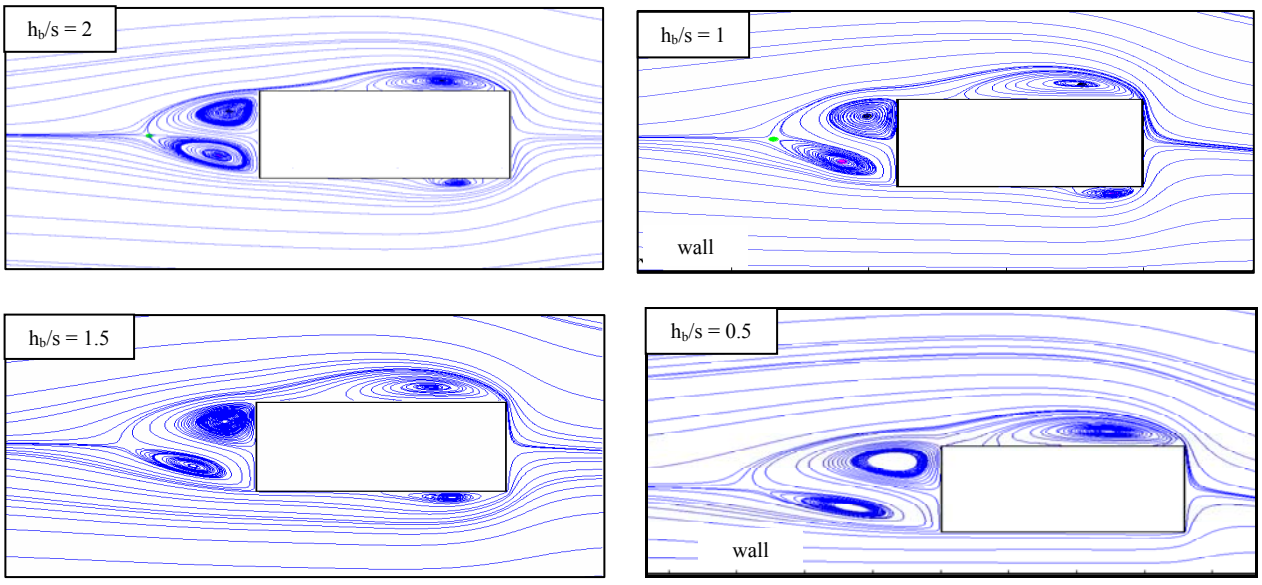


Fig. 8 Mean flow field numerical simulated for the various $h_b/s$ ratios considered

In the base region, the asymmetrical condition influences the dimension and disposition of the vortex structures: in particular, two comparable counter-rotating vortices are found for $h_b/s$ = 2; with the reduction of elevation of the cylinder the anti clockwise vortex is stretched downstream while the clock wise slightly increase its transversal dimension. This qualitative observation is confirmed by the detected position of vortex centers; for $h_b/s$ = 2 vortex centers are placed about at the same distance from the rear face of the cylinder, while the vortex nearer at the bottom wall is shifted downstream from the cylinder when the elevation is reduced.

Following we dealt with the quantitative characterization of the dimensionless parameters used by Blois and Malavasi [3]; moreover we comment the behaviors of the kinematic and dynamic dimensionless coefficient and where possible we compare our results with the experimental ones.

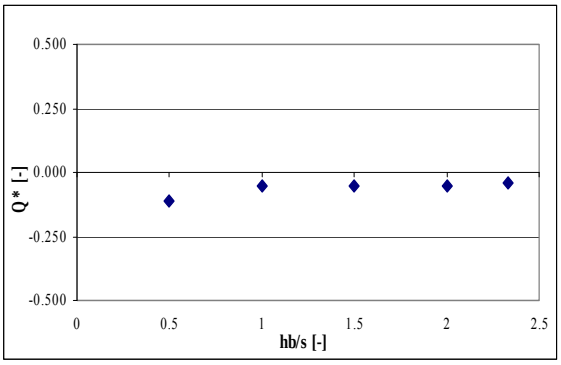


Fig. 9: Q* versus $h_b/s$

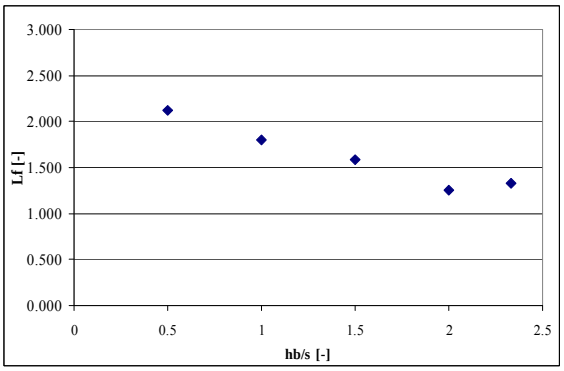


Fig. 10: Q* versus $h_b/s$; Lf versus $h_b/s$

Fig.(9) reports the dimensionless position of the stagnation point Q* on the front surface of the cylinder versus $h_b/s$. The value of this parameter remains almost constant for $h_b/s > 1$: in this condition the two causes of confinement produce a similar effect on the flow while a significant reduction occurs for $h_b/s=0.5$. The presence of the wall produces a sort of attraction causing a trend of Q* which agree with literature observation ([3]).
In the base region the parameter considered is formation length: this is a good indicator of the recirculation zone in rear face of the cylinder. As it can be noted from Fig.(10) the reduction of the distance between the intrados face of the cylinder and the bottom wall causes a progressive stretching of the recirculation zone and the parameter Lf encounters a progressive increase for $h_b/s<2$. This highlights how the presence of the bottom wall induces a stretching of the zone interested by the presence of the two counter-rotating vortices. In this zone the effect of the confinement is evident, with an increasing asymmetrical configuration of the flow.

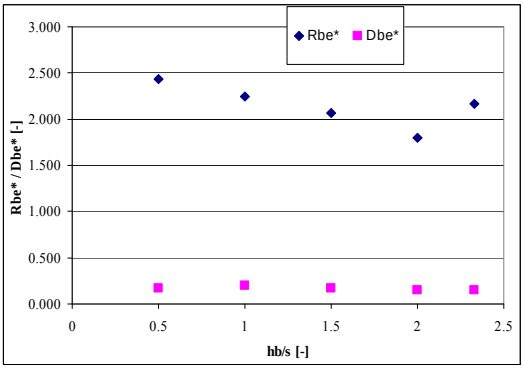


a)

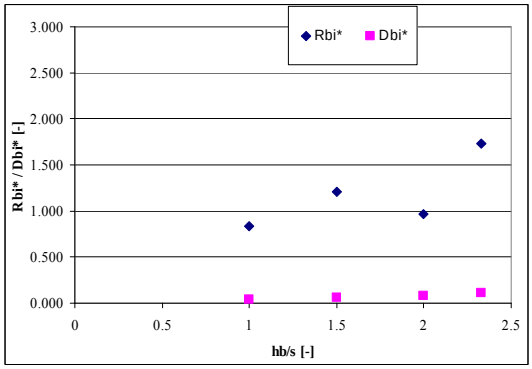


b)

Fig. 11: $R_b^*$ and $D_b^*$versus $h_b/s$, respectively at the a) extrados and b) intrados

Considering the reattachment point on the side surface of the cylinder (Fig.11), the first evidence is that in all the simulated cases reattachment along the extrados face of the cylinder occurs. A monotonic increase of the reattachment point is noted at the extrados for $h_b/s < 2$, while a general reduction of the same parameter in the intrados regions occurs.
Regarding the transversal size of the formation bubbles, both at the extrados and intrados the $D_b^*$ seems slightly affected by the presence of the wall in the range considered even if the $D_{be}^* > D_{bi}^*$. Finally we dealt with the evaluation of the pressure distribution around the obstacle and along the bottom wall.

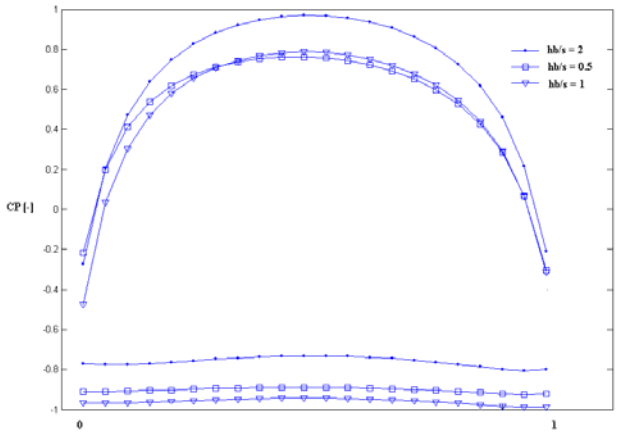


Fig. 12: Cp distribution on the frontal and rear face of the cylinder.

Particular consideration can be done for the frontal region (Fig.12): the simulated maximum of the stagnation pressure is for all the elevation considered almost in the middle of the frontal face. This fact confirms how the position of the stagnation point evaluated from the mean flow field elaboration slightly changes in the simulation. The reduction of the maximum and the distribution of pressure on the frontal face of the cylinder decreasing $h_b/s$ can be explained considering the influence of boundary layer thickness. Straatman and Martinuzzi [12] dealt with the evaluation of the influence of this parameter of the vortex shedding around a square cylinder closed to a confining wall. They highlight that the pressure distribution is affected by the boundary layer. In particular in the leading face as $\delta/s$ increases, the stagnation pressure decreases because proportionately more low momentum of fluid within the on-coming boundary layer impinges on the front face of the cylinder; moreover the thickening of the boundary layer results in an increase of the lift coefficient and a decrease of the drag coefficient.

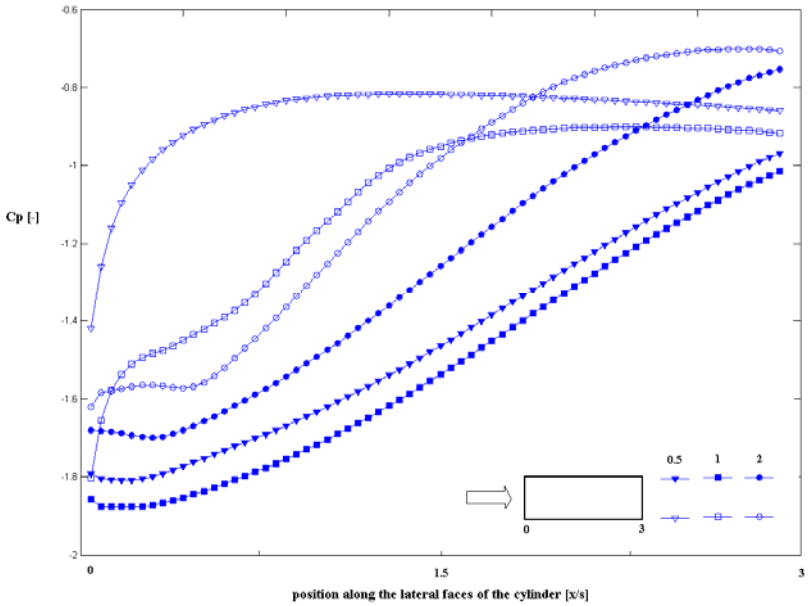


Fig. 13: Cp distribution along the lateral faces of the cylinder

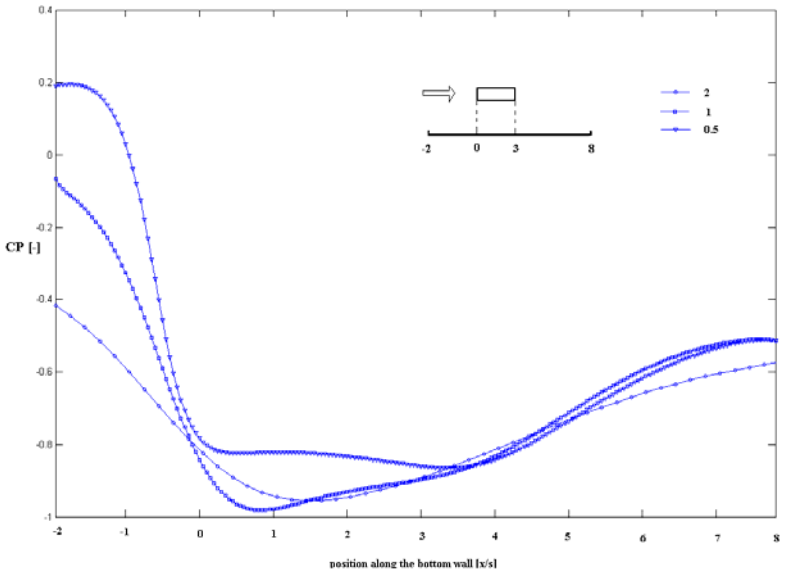


Fig. 14: Pressure distribution along the bottom wall.

In Fig.(13) and (14) are reported the pressure distribution at the lateral faces of the cylinder (Fig. 13) and along the bottom wall (Fig. 14). They highlight how the trend of the pressure radically changes when the elevation of the rectangular cylinder is reduced. As can be noted comparing the pressure distribution with the flow structures depicted in Fig.(8), the progressive vanishing of the vortex formation at the intrados region of the cylinder results in progressive increasing of the pressure along the bottom wall in the gap zone. The pressure distribution have a local minimum in the gap zone for $h_b/s=1$ and $h_b/s=2$, while a quasi-constant distribution is found for $h_b/s=0.5$ and a local minimum is shown out of the gap zone. Moreover for $h_b/s=0.5$ the pressure difference between the wall and the bottom face nearly vanishes.

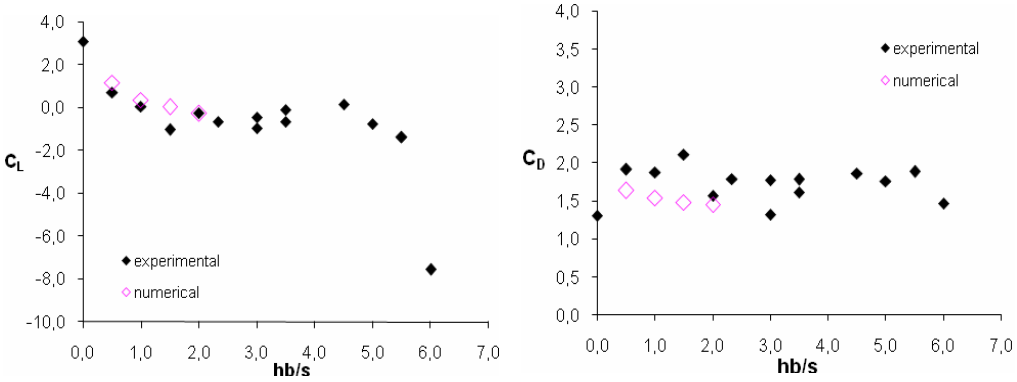


Fig. 15: Comparison of mean hydrodynamic coefficients. (experimental [1]; numerical [present work])

By considering the pressure distribution on the cylinder and the channel floor it is easier to give a physical motivation to the behavior of the force coefficients under the fluid-dynamic condition tested and help the interpretation of the experimental data. Fig.(15) provides the comparison between the force coefficient calculated by numerical simulation of flow and by direct force measurement [1]. In particular the increasing trend of both the lift and drag coefficient with the decreasing elevation of the cylinder is well reproduced. Slight differences on the quantitative value

of lift coefficient are found and the higher difference occurs for the elevation case $h_b/s=1.5$. In the experimental campaign this negative values seemed difficult to interpret and it is associated with an high experimental uncertainty ($u_{CL}=0.92$). The numerical simulation doesn't reproduce the negative pick, while a monotonic increase of the lift coefficient can be noted. The drag coefficient is underestimated in the range of $h_b/s$ considered, however the majority of simulated values fall in the uncertainty range of the measured values. Especially in this case the numerical simulation gives useful information to find out the physical trend of $C_D$ versus $h_b/s$.

## 4 CONCLUSIONS

In present work a numerical procedure for the simulation of the dynamic loading on a rectangular cylinder placed in a stationary flow has been validated and used to study the effect of an asymmetrical confined flow on the same cylinder. The good reproduction of the experimental data both in dynamic and cinematic terms has certificate the reliability of the validated numerical approach.

In this work experimental consideration about the asymmetrical flow condition performed on the cylinder has been integrate with additional information. In particular results from the numerical simulation have suggested significant interpretation of the phenomena involved. The mean flow field characterization has shown the sensible distortion of the vortex structures in all the regions around the cylinder. It has been evidenced how the pressure distribution in the gap zone (between the intrados face of the cylinder and the bottom wall) highly changes when the cylinder is brought closed to the wall: the reduction of the vortex shedding which occurs for $h_b/s = 0.5$ is accompanied by a raising of the pressure in that zone; moreover the pressure distribution along the bottom wall and intrados face of the cylinder are almost the same. Similarities have been found with the flow around a square cylinder in the same condition but, since the different flow mechanism involved mainly due to the different aspect ratio, the simulation have highlighted how the influence of the bottom wall on the rectangular cylinder yet occurs for relative higher elevation from the same wall.

The numerical approach described in this paper has shown good results in terms of reproducibility of the experimental evidence and prediction of complex flow characteristics; the validated procedure has even permitted to reach a reasonable simulation time (almost two days for each case simulated) and good reliability of the numerical results.

## ACKNOWLEDGMENTS

The numerical simulations used in this paper are run using a FLOW-3D® license provided by XC-Engineering within the agreement between the D.I.I.A.R. of Potitecnico di Milano and the XC-Engineering. We especially thank Stefano Mascetti for his suggestions and help in the optimization of simulation set-up.

## REFERENCES

[1] S. Malavasi, A. Guadagnini. Interactions between a rectangular cylinder and a free-surface flow. *Journal of Fluids and Structure*, 23, 1137–1148, 2007.

[2] A. Cigada et. al. Effects of an asymmetrical confined flow on a rectangular cylinder. *Journal of Fluids and Structure*, 22, 213–227, 2007.

[3] G. Blois, S. Malavasi. Flow structure around a rectangular cylinder near a solid surface. XVIII AIMETA Conference, Brescia, Italy, September 11-14, 2007.

[4] A. Okajima. Flow around a rectangular cylinder with a section of various depth/breath ratios. *Journal of Wind Engineering*, 17, 79-80, 1983

[5] K. Shimada, T. Ishihara. Application of a modified k-epsilon model to the prediction of aerodynamic characteristics of rectangular cross-section cylinders. *Journal of Fluids and Structure*, 16, 465–485, 2002.

[6] D. Yu, A. Kareem. Parametric study of flow around rectangular prisms using LES. *Journal of Wind Engineering and Industrial Aerodynamics*, 77, 653–662, 1998.

[7] B.A. Younis, V.P. Przulj. Computation of turbulent vortex shedding. *Computational Mechanics*, 37, 408-425, 2006.

[8] G. Bosh, W. Rodi. Simulation of vortex shedding past a square cylinder near a wall. *Int. Journal of Heat and Fluid Flow*, 17, 267-275, 1996.

[9] R.J. Martinuzzi, S.C.C. Bailey, G.A. Kopp. Influence of wall proximity on vortex shedding from a square cylinder. *Experiments in Fluids*, 34, 585-596, 2003.

[10] A.G. Straatman and R. J. Martinuzzi. A comparison of second-moment closure models in the prediction of vortex shedding from a square cylinder near a wall. ASME *Journal of Fluids Engineering,* 124(3), 2002

[11] A.G. Straatman and R. J. Martinuzzi. An examination of the effects of boundary layer thickness on vortex shedding from a square cylinder near a wall. *Journal of Wind Engineering and Industrial Aerodynamics,* 91, 1023-1037, 2003

[12] G.Iaccarino, A.Ooi, P.A. Durbin, M. Behnia. Reynolds averaged simulation of unsteady separated flow. *Int. Journal of Heat and Fluid Flow,* 24, 147-156, 2003.